CHEMISTRY
A EUROPEAN JOURNAL

Design of Organic Semiconductors: Tuning the Electronic Properties of π-Conjugated Oligothiophenes with the 3,4-Ethylenedioxythiophene (EDOT) Building Block

Mathieu Turbiez,[a] Pierre Frère,*[a] Magali Allain,[b] Christine Videlot,[c] Jörg Ackermann,[d] and Jean Roncali*[a]

Abstract: Hybrid oligothiophenes based on a various combinations of thiophene and 3,4-ethylenedioxythiophene (EDOT) groups have been synthesized. UV/Vis absorption spectra show that the number and relative positions of the EDOT groups considerably affect the width of the HOMO–LUMO gap and the rigidity of the conjugated system. Analysis of the crystallographic structure of two hybrid quaterthiophenes confirms that insertion of two adjacent EDOT units in the middle of the molecule leads to a self-rigidification of the conjugated systems by intramolecular S···O interactions. Cyclic voltammetry data shows that the first oxidation potential of the oligomers decreases with increasing chain length and increasing number of EDOT groups for a given chain length. Electrochemical studies and theoretical calculations show that the positions of the EDOT units in the conjugated chain control the potential difference (ΔE_p) between the first and second oxidation steps. Moving the EDOT groups from the outer to the inner positions of the conjugated system increases ΔE_p. Theoretical calculations confirm that this phenomenon reflects an increase of the intramolecular coulombic repulsion between positive charges in the dication. A thin-film field-effect transistor was fabricated by vacuum sublimation of a pentamer with alternating thiophene–EDOT structure, and the hole mobility was determined.

Keywords: 3,4-ethylenedioxythiophene · oligothiophenes · pi interactions · semiconductors · structure–property relationships

Introduction

Thiophene-based π-conjugated oligomers are subject to intensive work focused on their use as organic semiconductors in devices such as thin-film organic field-effect transistors (OFET),[1] electroluminescent diodes (OLED),[2] and photovoltaic cells.[3]

Although each type of device requires the optimization of specific properties such as oxidation and reduction potential, absorption and emission spectrum, or luminescence efficiency, in all cases the final output performance of the device strongly depends on the charge-transport efficiency of the active material.

The intrinsic conductivity of organic semiconductors based on π-conjugated structures depends on the concentration and mobility of the charge carriers. Besides intermolecular factors which determine the transfer integral between neighboring molecules,[4] the electronic structure of the conjugated system also plays a key role in the final performance of the corresponding semiconductor. In fact, quantities such as ionization potential, electron affinity, and band gap,

[a] Dr. M. Turbiez, Prof. P. Frère, Dr. J. Roncali
Groupe Systèmes Conjugués Linéaires, CIMMA, UMR CNRS 6200
Université d'Angers, 2 Boulevard Lavoisier, 49045 Angers (France)
Fax: (+33) 241-735-405
E-mail: pierre.frere@univ-angers.fr
jean.roncali@univ-angers.fr

[b] Dr. M. Allain
CIMMA, UMR CNRS 6200, Université d'Angers
2 Boulevard Lavoisier, 49045 Angers (France)

[c] Dr. C. Videlot
Laboratoire des Matériaux Moléculaires et des Biomatériaux
UMR CNRS 6114, Université de la Méditerranée
163 Avenue de Luminy, 13288 Marseille (France)

[d] Dr. J. Ackermann
Centre de Recherche de la Matière Condensée et des Nanosciences
UPR 725, Université de la Méditerranée
163 Avenue de Luminy, 13288 Marseille (France)

Supporting information for this article is available on the WWW under http://www.chemeurj.org/ or from the author.

DOI: 10.1002/chem.200401058

which control the injection of holes and/or electrons in the material and the thermal population of the conduction band at ambient temperature, depend on the HOMO and LUMO energy levels of the elemental conjugated unit and on their difference.[5]

We have shown already that besides its strong electron-donor properties,[6] 3,4-ethylenedioxythiophene (EDOT) can give rise to noncovalent intramolecular interactions with adjacent thiophenic units and thus induce self-rigidification of the π-conjugated system in which it is incorporated.[7–9] Although this property has been applied to the design of low-band-gap polymers,[7] push–pull NLO-phores,[8] and extended tetrathiafulvalene analogues,[9] the use of EDOT as building block in π-conjugated oligomers potentially usable as organic semiconductors has not been considered so far.

The EDOT dimer[10] and trimer[11] were reported some years ago. More recently, EDOT oligomers end-capped with mesitylthio,[12a] phenyl,[12b] or hexyl chains[12c] have been synthesized. However, until now chain length has been limited to the tetramer because of the instability of longer oligomers. A possible way to circumvent this obstacle is the synthesis of more stable hybrid EDOT–thiophene oligomers.[13]

Here we describe the synthesis of new series of hybrid EDOT–thiophene oligomers in which the number and/or position of the EDOT groups have been systematically varied (Scheme 1). The structure and electronic properties of these various series of oligomers were analyzed by X-ray diffraction, optical and electrochemical techniques, and theoretical calculations. The results are discussed with regard to the influence of the number and positions of the EDOT groups in the structure and electronic properties of the π-conjugated system. On the basis of some conclusions of these investigations, a first prototype OFET based on a pentamer with an alternating T–E structure was fabricated and characterized.

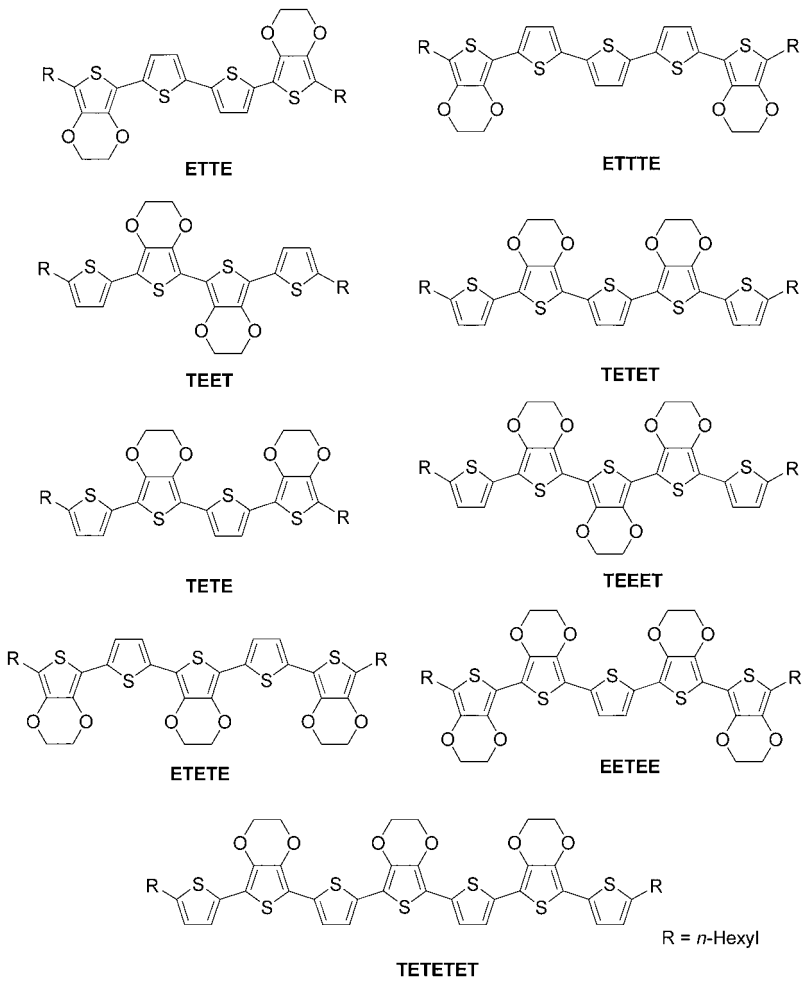

Scheme 1. Structures of the hybrid oligomers (E = EDOT, T = thiophene).

Results and Discussion

Synthesis: All oligomers were constructed from a few building blocks, the synthesis of which is presented in Scheme 2. EDOT (**1**) was converted to mono- and distannyl derivatives **1b** and **1c** by treatment with *n*BuLi then Bu_3SnCl. These stannyl compounds were then subjected to Stille coupling with 2-bromothiophene or 2-bromo-5-hexylthiophene to give dimers **2a** and **3a** and trimer **4a** in 33–73% yield. Treatment of **4a** with two equivalents of *N*-bromosuccinimide (NBS) afforded dibromo derivative **4b** in 82% yield. Bis-EDOT **5a** was obtained by oxidative coupling of the lithiated derivative of **1** in the presence of $CuCl_2$.[10a,14] Addition of a slight excess of bromohexane to the monolithiated derivative of **5a** led to a mixture of the desired 2-hexyl-bis-EDOT **6a** with **5a** and the disubstituted compound. This phenomenon, already observed on application of the same procedure to **1**, which led to a mixture of 2-*n*-hexyl- (**7a**), 2,5-di-*n*-hexyl-, and unsubstituted EDOT, was interpreted by proton exchange between the lithiated and monosubstituted derivatives.[12c] Compound **7a** was isolated by distillation under reduced pressure, while **6a** was separated by

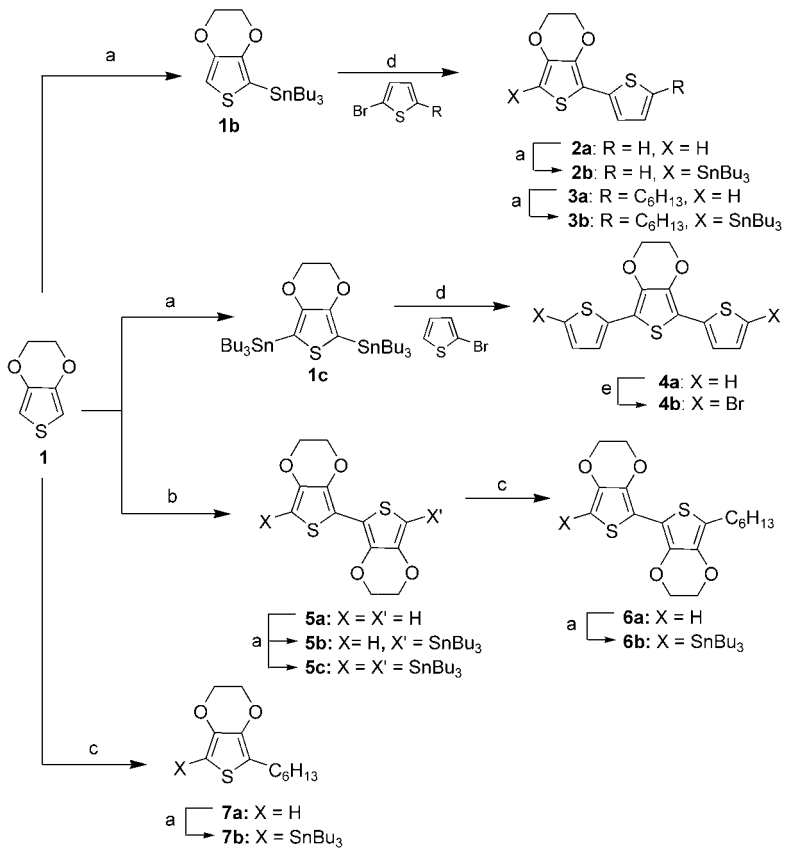

Scheme 2. Synthesis of the building blocks. a) *n*BuLi then Bu_3SnCl; b) *n*BuLi then $CuCl_2$; c) *n*BuLi then *n*-bromohexane; d) $[Pd(PPh_3)_4]$; e) NBS/DMF.

column chromatography on silica gel because of its instability at high temperature.

All target oligomers were then assembled by Stille coupling in the presence of a palladium catalyst (Scheme 3). To this end, compounds **2a**, **3a**, **5a**, **6a**, and **7a** were converted to the corresponding monostannyl derivatives **2b**, **3b**, **5b**, **6b**, and **7b**, respectively, and to the distannyl compound **5c** for bis-EDOT **5a**. All these reagents were quickly used after flash chromatography.

Because of the instability of mono- or dibromo-EDOT and bis-EDOT,[15] these compounds were avoided as much as possible, and most of the Stille coupling reactions involved mono- or distannyl-EDOT and di-EDOT and mono- or dibromo derivatives of the thiophenic building blocks, namely, mono-, bi-, or terthiophene (Scheme 3). Thus, **TEET** was prepared in 56% yield by coupling distannyl derivative **5c** with a slight excess of 2-hexyl-5-bromothiophene. Similarly, **ETTE** was obtained in 70% yield by coupling of **7b** with 5,5′-dibromo-2,2′-bithiophene.

The synthesis of the alternating tetramer **ETET** involved first coupling of **2b** with 2-hexyl-5-bromothiophene to afford trimer **8a** in 55% yield. This compound was then converted to bromo derivative **8b** with NBS in chloroform (28% yield). A second Stille coupling between stannyl compound **7b** and **8b** gave the target compound **ETET** in 10% yield. The low yields of the last two steps are due to the low stability of **8b**, which undergoes rapid degradation at room temperature.

The pentamer **ETTTE** was prepared in 40% yield by a twofold Stille reaction between **7b** and dibromoterthiophene. Similarly, alternating **ETETE** was obtained in 47% yield by coupling **7b** with dibromo trimer **4b. TETET** and **TEEET** were synthesized by coupling **3b** with dibromothiophene (**9**) or dibromo-EDOT. **TETET** and **TEEET** were obtained in 62 and 21% yield, respectively. The low yield for **TEEET** was due to instability of dibromo-EDOT. Pentamer **EETEE** was obtained in 20% yield by coupling the stannyl derivative **5c** with **9**. It is noteworthy that attempts to replace dibromothiophene by dibromo-EDOT in order to obtain penta-EDOT led only to degradation products, and thus end-capped tetra-EDOTs remain until now the longest known EDOT oligomers.[12b,c] Finally, coupling **3b** with **4b** gave the heptamer **TETETET**, which is the longest EDOT-containing conjugated oligomer known to date. Unfortunately, due to its very low solubility, this compound could not be completely purified.

Crystallographic structures: The crystallographic structures of single crystals of tetramers **ETTE** and **TEET** obtained by slow evaporation of chloroform/ethanol solutions were analyzed by X-ray diffraction. The conformations adopted by **ETTE** and **TEET** reveal significant differences in the orientation of the sulfur atoms of the two median adjacent thiophenes (*anti* or *syn*). **TEET** crystallizes in the monoclinic space group $P2_1/n$ and the structure is defined by a half molecule due to an inversion center (Figure 1, top). The four thiophene rings adopt an *anti* conformation. The median di-EDOT block has a fully planar geometry, and the distance between the sulfur atom and the oxygen atom of the adjacent EDOT ring is considerably shorter than the sum of the van der Waals radii of sulfur and oxygen (2.91 versus 3.35 Å). This short distance indicates noncovalent intramolecular interactions which rigidify the central part of the molecule. Sulfur–oxygen interactions are also observed between the end thiophenes and the neighboring EDOT rings. However, the S···O distances (3.10 Å) are slightly larger than those observed for the median EDOT groups. This result and the 13° dihedral angle between the terminal thio-

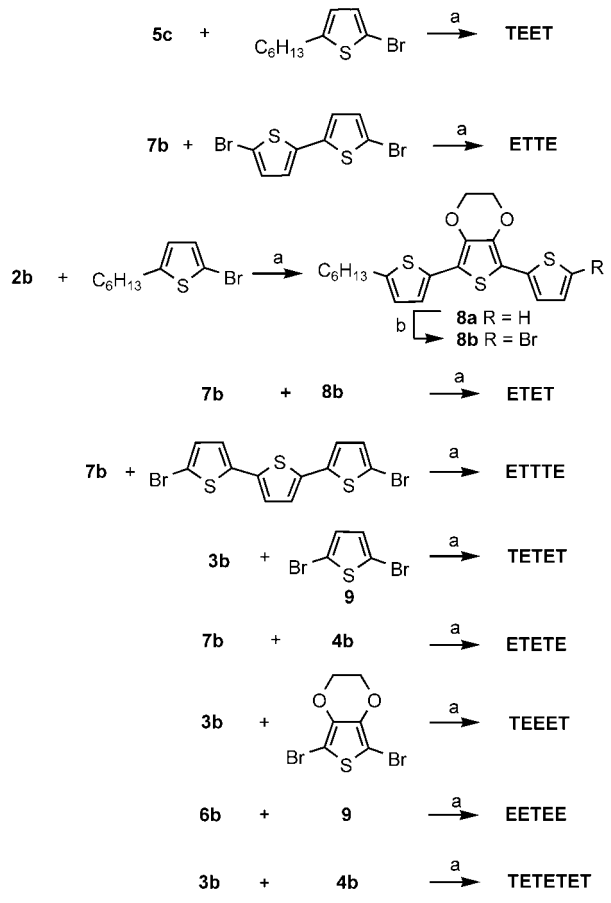

Scheme 3. Synthesis of the oligomers a) $[Pd(PPh_3)_4]$; b) NBS/DMF.

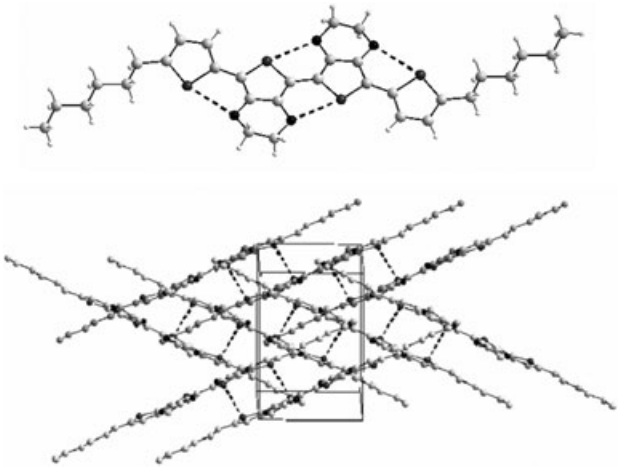

Figure 1. Crystal structure of **TEET**. Top: molecular structure. Bottom: packing mode. S···O and S···S intra- and intermolecular interactions are represented by dotted lines.

phene and EDOT show that S···O interactions are weaker than between the two median EDOT units.

As shown in Figure 1 (bottom), the molecules stack along two axes at an angle of 60°. In each column the molecules overlap with superposition of two thiophene rings with intermolecular distances of 3.98 Å.

ETTE crystallizes in the triclinic space group $P\bar{1}$ and the structure is defined by an independent molecule (Figure 2). Although the terminal EDOT units are in *anti* conformation

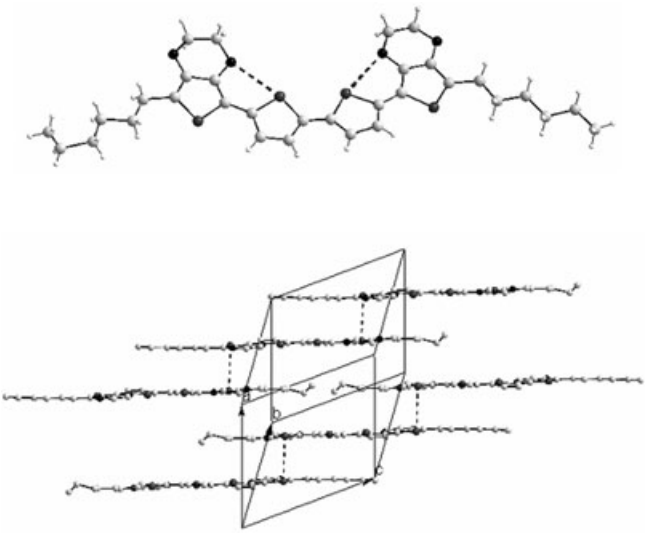

Figure 2. Crystal structure of **ETTE**. Top: molecular structure. Bottom: packing mode. S···O and S···S intra- and intermolecular interactions are represented by dotted lines.

stabilized by two S···O interactions ($d = 3.02$, 2.96 Å) the two median thiophene rings have a *syn* orientation with a dihedral angle significantly larger than that between the end EDOT groups and the adjacent thiophenes (12 versus 5°, respectively). The molecules stack along the *b* axis with overlap limited to the terminal EDOT rings and intermolecular distances of 3.5 Å (Figure 2, bottom).

The crystal structures of the two compounds show that in both cases the EDOT blocks strongly affect the geometry of the π-conjugated system through intramolecular S···O interactions. This effect is particularly intense when two EDOT groups are adjacent. On the other hand, the quite different molecular organizations found in the two crystal structures show that the EDOT unit significantly affects intermolecular interactions. In this regard, the cofacial overlap of EDOT groups observed in the **ETTE** crystal could represent a positive factor for high hole mobility.

Very thin single crystals of pentamer **TETET** were also obtained. Although the quality of the crystals did not allow full structural resolution due to the imprecise positioning of the alkyl carbon atoms, all atoms of the π-conjugated chain are well positioned and show that the five thiophene rings adopt a fully planar all-*anti* conformation.

Optical properties: Electronic absorption and fluorescence emission spectra of the oligomers were investigated in dichloromethane, and the results are listed in Table 1. The data for tetrathiophene (**4T**)[16] and tetra-EDOT (**4E**) endcapped with *n*-hexyl chains are also included for comparison.[12c]

Table 1. Optical spectroscopic data of oligomers in CH_2Cl_2.

Compound	λ_{max} [nm][a]	λ_{em} [nm][b]	Φ[c]
4T[d]	402	462, 492	17.4
ETTE	422	476, 503	18.0
ETET	425	474, 504	14.8
TEET	424	466, 497	12.8
4E[e]	430	471, 502	13.3
ETTTE	445	508, 539	24.7
TETET	452	503, 537	28.0
TEEET	454	502, 537	18.0
ETETE	455	509, 542	26.5
EETEE	462	513, 545	26.0
TETETET	488	–	–

[a] Wavelength absorption maxima, 10^{-5} M in CH_2Cl_2. [b] Fluorescence emission band, 10^{-6} M in CH_2Cl_2. [c] Fluorescence quantum yield determined using perylene as standard. [d] From reference [16]. [e] From reference [12c].

Figure 3 compares the UV/Vis absorption and emission spectra of **ETTE** and **TEET** to those of the pure thiophene (**4T**) or EDOT (**4E**) tetramers. As expected, increasing the number of EDOT groups in the chain produces a red shift of λ_{max} and hence a narrowing of the HOMO–LUMO gap (Table 1). Figure 3 shows that **4T** exhibits a broad and structureless spectrum due to the rotational freedom of the thiophene rings, while the spectrum of **4E** displays a well resolved vibronic fine structure characteristic of rigid conjugated systems. The quasiconstant energy spacing between the three maxima (1300–1400 cm^{-1}) is consistent with a C=C stretching mode in the heteroaromatic moieties, strongly coupled to the electronic structure.[17] Between the two limiting cases of **4T** and **4E**, the spectrum of **ETTE** shows that replacement of the two terminal thiophenes by EDOT units results in the emergence of a discernible fine structure. This fine structure becomes better resolved when the conjugated chain contains alternating EDOT–thiophene sequences (**ETET**, see Figure 4 below) or a central bi-EDOT group (**TEET**). This result confirms, in agreement with the crystallographic data, that intramolecular S···O interactions are maximized when EDOT groups are adjacent. As can be seen in Figure 3, all oligomers have rather similar fluorescence emission spectra with well-resolved vibronic fine structure. This similarity can be explained by the fact that, contrary to the ground state, for all compounds the first singlet excited state is expected to adopt a quinonoid planar rigid geometry. On the other hand, the decrease in the Stokes shift observed when the number of EDOT groups in the conjugated chain increases, suggests a lesser degree of structural reorganization between the ground state and the first excited state. This is consistent with a more rigid ground state due to S···O interactions.

Similar effects are observed for the pentamers, and comparison of the spectra of pentamers containing two EDOT groups (**ETTTE** and **TETET**; not shown) shows that moving the two EDOT groups towards the middle of the conjugated chain enhances the resolution of the vibronic fine structure and causes a red shift of λ_{max} from 445 to 452 nm. Similarly, the spectra of pentamers containing three EDOT groups reveal better resolved fine structure for **TEEET** than for the alternating **ETETE** although the two molecules have practically the same λ_{max} (455 nm). Again, the fluorescence emission spectra reveal a smaller Stokes shift for **TEEET** than for **ETETE**, consistent with less structural reorganization on photoexcitation due to a more rigid ground-state geometry.

As expected, the pentamer containing four EDOT units **EETEE** has the most red shifted λ_{max} (462 nm) and smallest HOMO–LUMO gap of the series.

These various results show that incorporation of EDOT units in *n*Ts allows modulation of the geometry and HOMO–LUMO gap of the conjugated systems by means of a synergistic combination of electronic and self-rigidification effects.

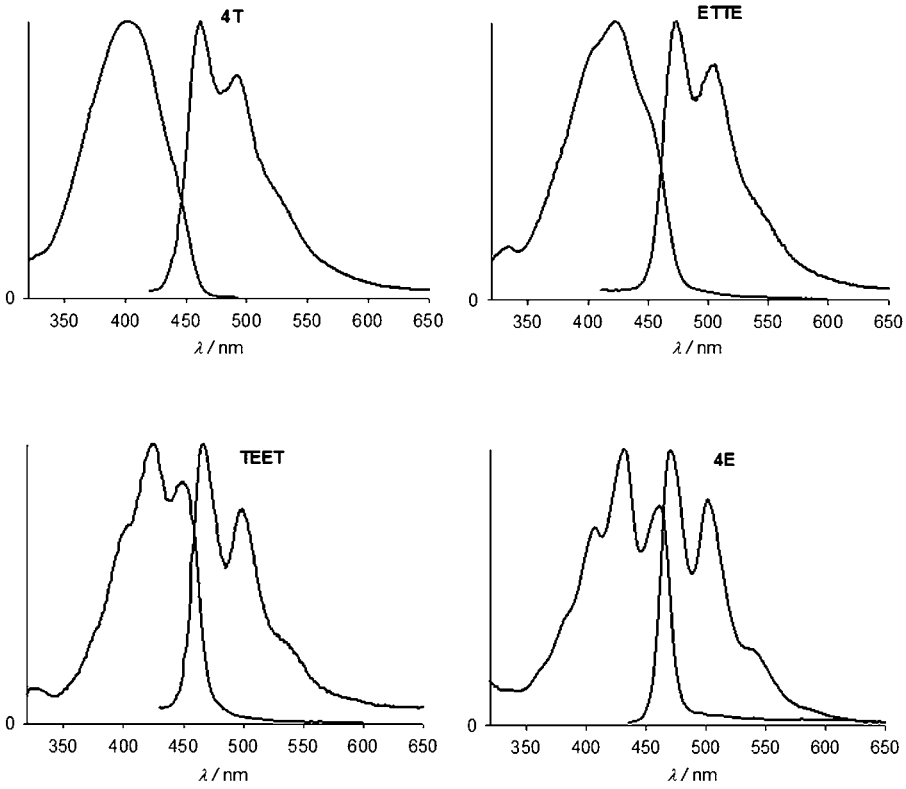

Figure 3. Normalized absorption and emission spectra of tetramers **4T**, **ETTE**, **TEET**, and **4E** in CH_2Cl_2.

However the latter effect strongly depends on the position of the EDOT groups in the chain; the maximum effect is observed for adjacent EDOT blocks in the middle of the conjugated structure. Thus, a regular alternation of thiophene and EDOT rings can represent a good trade-off for improving π-electronic delocalization by spreading the self-structuring effect of the EDOT group over the whole oligothiophene chain. This conclusion is supported by the absorption spectra of oligomers based on a regular alternating thiophene–EDOT structure, which show that lengthening of the conjugated chain from four to seven rings produces a steady red shift of the spectrum without alteration of the fine structure (Figure 4). This result confirms that the self-rigidification associated with intramolecular S···O interactions can have a coherence length of at least seven thiophene units.

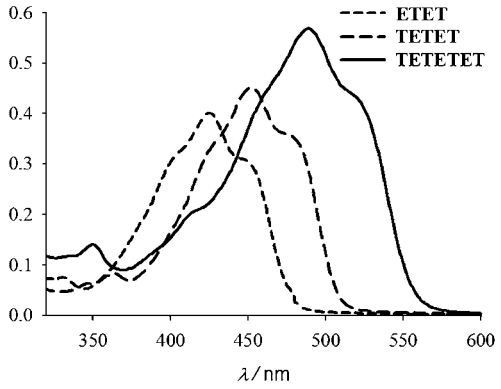

Figure 4. UV/Vis absorption spectra of alternating oligomers **ETET**, **TETET**, and **TETETET** in CH_2Cl_2.

Theoretical calculations: To analyze in more detail the influence of EDOT on the electronic properties of hybrid oligothiophenes, theoretical calculations were performed at the ab initio density functional level with the Gaussian 98 package.[18] Becke's three-parameter gradient-corrected functional (B3LYP) with a polarized 6-31G* basis was used for full geometry optimization of the tetramers. The *n*-hexyl substituents were not considered to limit computation time. The calculated HOMO and LUMO levels are gathered in Table 2. Although **TEET** and **TETE** (see Supporting Information) show a fully planar conformation, a slight dihedral angle of 13° is observed for the central bithiophene unit of **ETTE**. Coplanarity of the EDOT units with the adjacent thiophene rings is associated with short intramolecular S···O distances (ca. 3.1 Å), slightly larger than those found in the X-ray structures of **TEET** and **ETTE**. The calculations for a *syn* orientation of the central bithiophene of **ETTE** leads also to a dihedral angle of 13–15°, which is very close to that observed in the crystal structure (Figure 2). By contrast, for **TEET** in a *syn* orientation the dihedral angle between the EDOT units is strongly increased to 30°. The LUMO energy level is constant for the three isomers (−1.58 eV), whereas the HOMO level is higher when the EDOT groups occupy the inner positions of the conjugated chain. Consequently, **TEET** has a smaller HOMO–LUMO gap ΔE than **ETTE**. As expected, the ΔE values for all hybrid oligomers lie between those of the two limiting cases **4T** and **4E**.

Table 2. HOMO/LUMO energy levels and gap ΔE calculated by DFT method (B3LYP/6-31G*).

	HOMO [eV]	LUMO [eV]	ΔE [eV]
4T	−5.00	−1.87	3.13
ETTE	−4.59	−1.58	3.01
ETET	−4.53	−1.58	2.95
TEET	−4.50	−1.58	2.92
4E	−4.17	−1.29	2.88
ETTTE	−4.54	−1.75	2.79
TETET	−4.45	−1.75	2.70
ETETE	−4.35	−1.65	2.70
TEEET	−4.27	−1.61	2.66
EETEE	−4.18	−1.51	2.67

The molecular orbital analysis of **TEET** shows that the oxygen atoms have a small contribution of the atomic orbital coefficient to the HOMO level, which indicates a possible mesomeric effect of the ether group (see Supporting Information). In contrast, for **ETTE** no contribution of the external O atoms or adjacent C atoms is observed. For the alternating **ETET**, only the inner O atom of the terminal EDOT group makes some contribution to the HOMO level. Calculated data for the pentamers show that, as expected, ΔE decreases with increasing number of EDOT units. However, here again the position of the EDOT groups has a decisive effect. Thus, whereas the largest ΔE value of 2.79 eV is observed for **ETTTE** with two external EDOT units, **TETET** and **ETETE** show the same gap (2.70 eV) despite the presence of a third EDOT group in the latter case. The effect of this additional EDOT unit is a 0.10 eV shift of both the HOMO and LUMO levels. Comparison of the data for **ETETE** and **TEEET** shows that regrouping the three EDOT groups in the middle of the molecule produces a further decrease in ΔE with a larger shift of the HOMO level than for the LUMO. Finally, introduction of a fourth EDOT group leads to a further increase in the HOMO but has no effect on ΔE due to the parallel shift of the LUMO. This latter result appears particularly demonstrative of the key role played by the position of the EDOT groups in the control of the electronic properties.

Electrochemical properties: The electrochemical properties of the various oligomers were analyzed by cyclic voltammetry in dichloromethane with Bu_4NPF_6 as supporting electrolyte. The data are summarized in Table 3. The CV of all oligomers shows two reversible one-electron processes corresponding to the successive formation of the radical cation and dication (Figure 5). As expected, for both series progressive replacement of thiophene by EDOT in the conjugated system leads to a negative shift of the first anodic peak potential E_{p1} due to the donor effect of EDOT. For all oligomers E_{p1} values are in excellent agreement with the calculated HOMO levels (Table 2). Comparison of the data

Table 3. Cyclic voltammetric data[a] for oligomers.

Compound	E_{p1} [V]	E_{p2} [V]	ΔE_p [mV]
4T[b]	0.85	1.14	290
ETTE	0.57	0.84	270
ETET	0.56	0.90	340
TEET	0.48	0.92	440
4E[b]	0.22	0.62	400
ETTTE	0.60	0.80	200
TETET	0.50	0.80	300
ETETE	0.44	0.69	250
TEEET	0.37	0.71	340
EETEE	0.31	0.59	280

[a] 10^{-4} M in 0.1 M Bu_4NPF_6/CH_2Cl_2, scan rate 100 mV s^{-1}, reference AgCl/Ag. [b] From reference [12c].

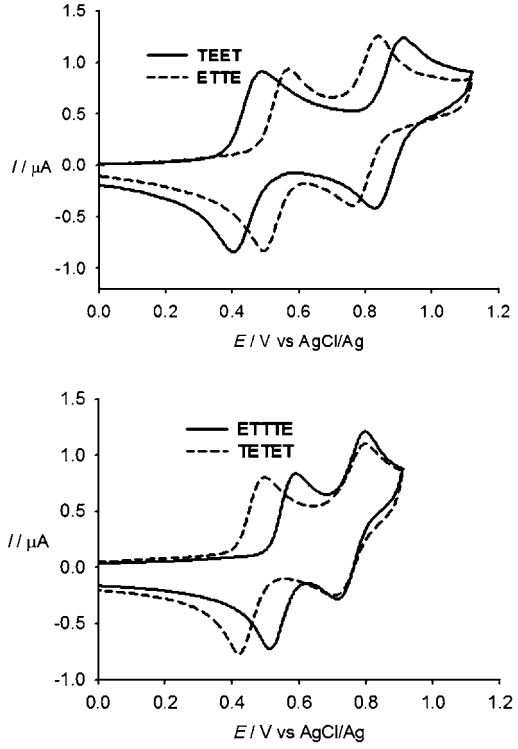

Figure 5. Cyclic voltammograms of the oligomers (10^{-4} M) in 0.10 M Bu_4NPF_6/CH_2Cl_2, scan rate 100 mV s^{-1}. Top: **ETTE** and **TEET**; bottom: **ETTTE** and **TETET**.

within each series shows that the position of the EDOT group strongly affects the E_{p1} value. For the tetramers the lowest E_{p1} value of 0.48 V is found when the EDOT groups are at the inner positions (**TEET**; cf. 0.57 V for **ETTE**). As expected, both E_{p1} values lie between those of the two limiting cases **4T** and **4E** ($E_{p1}=0.85$ and 0.22 V, respectively). The same trend is observed in the pentamer series, and comparison of the data for **ETTTE** and **TETET** reveals a 100 mV negative shift of E_{p1} for the latter. Similarly E_{p1} undergoes a 70 mV negative shift when the three EDOT groups of **ETETE** are gathered in the middle of the molecule in **TEEET**. As expected, introduction of an additional EDOT group (**EETEE**) leads to a further decrease of E_{p1} to 0.31 V. As can be seen in Table 3 and Figure 5, the potential difference between the first and second oxidation $\Delta E_p = E_{p2} - E_{p1}$ shows a marked dependence on the position of the EDOT units in the chain. For both series of oligomers, moving the EDOT units from the outer to the inner positions of the π-conjugated chain produces a marked increase of ΔE_p, for example, 140 mV between **ETTE** and **TEET**, 100 mV between **ETTTE** and **TETET**, and 90 mV between **ETETE** and **TEEET** (Table 3). The difference ΔE_p reflects the coulombic repulsion between positive charges in the dicationic state. On this basis, the above results show that the coulombic repulsion (and hence the difficulty to stabilize the dication) increases when the EDOT units move to the inner part of the π-conjugated chain. Such a behavior, already observed for conjugated systems based on EDOT or bis-EDOT[9,12a] can be attributed to localization and stabilization of the positive charges on the EDOT-rich part of the structure. It is noteworthy that ΔE_p decreases by 40 mV between **TEET** and **4E**. This results shows that the more homogeneous electronic distribution in a purely EDOT-based conjugated system allows better delocalization of the positive charges of the dication than in the hybrid **TEET**.

To gain a deeper insight into the effect of EDOT on the charge distribution of the dication, optimization of the dications of **4T**, **ETTE**, **TEET**, and **4E** was performed. Calculations were done with the same B3LYP functional as for neutral states and also with the U-B3LYP method by considering singlet and triplet states, respectively. As expected for short oligomers, the dications have higher bipolaron than biradical character with total singlet–triplet state energy differences of about 14 kcal. For the singlet state of each molecule, geometric optimization with U-B3LYP led to fully identical results to those obtained with the restricted functional.

Oligomers were considered in the all-*anti* conformation and hexyl groups were not included. In each case, the structure was found to be fully planar. The net charges for the thiophene or EDOT units, calculated by summing the Mulliken charges of the atoms forming the rings,[19] are listed in Table 4. For homogeneous **4T** and **4E**, the global charge is rather evenly distributed over the whole conjugated system with a slight excess ΔQ on the terminal rings. Quite different results are obtained for the hybrid systems. Thus, **ETTE** has a larger excess of charge on the terminal rings than **4T** and **4E**, while for **TEET** the excess charge is located on the central di-EDOT block. These results, which agree well with the ΔE_p values in Table 3, further support a preferential lo-

Table 4. Mulliken net charges for the thiophene and EDOT units calculated at the B3LYP/6-31G* level for tetramers. ΔQ corresponds to the difference between the charges of terminal and central rings.

	Terminal rings	Central rings	ΔQ
4T	0.56	0.44	+0.12
ETTE	0.61	0.39	+0.22
TEET	0.48	0.52	−0.04
4E	0.54	0.46	+0.08

calization of the positive charge on the EDOT-rich part of the hybrid π-conjugated chains.

Oxidation of *n*Ts to the cation radical and dication results in a transition from an aromatic to a quinonoid structure with inversion of the single and double bonds (Scheme 4).

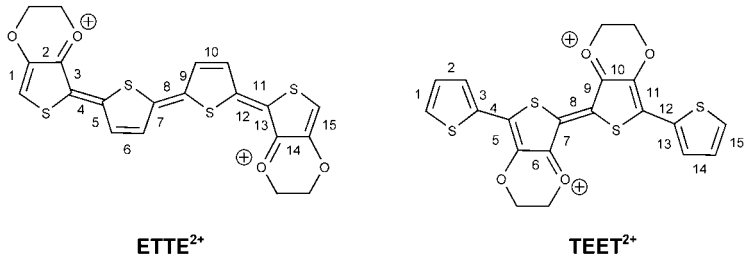

ETTE^{2+} **TEET**$^{2+}$

Scheme 4. Structure and bond numbering of dications **ETTE**$^{2+}$ and **TEET**$^{2+}$.

In fact, such a quinonoid structure has been observed in crystals of dication salts of tetra- and hexathiophene.[20] The differences δl between the bond lengths of the neutral and dication states (using the same base for optimization) allow the geometrical changes of the conjugated chain associated with the formation of the dication to be visualized. Figure 6

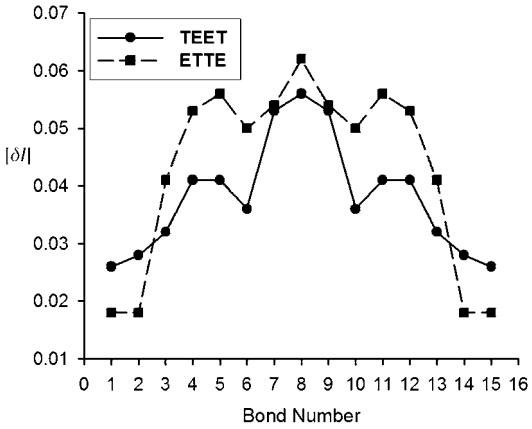

Figure 6. Difference $|\delta l|$ [Å] between the optimized bond lengths (B3LYP/6-31G*) of the neutral and dication species.

shows the variation $|\delta l|$ for each bond for **ETTE** and **TEET** (see Scheme 4 for bond numbering). For **ETTE** the largest changes involve bonds 3–5 and 11–13, indicating that the charges are essentially localized at the ends of the molecule. In contrast, for **TEET** the largest differences are observed for bonds 7–9, in agreement with preferential charge localization in the middle of the molecule. Furthermore, comparison of the C–O bond lengths in the neutral and dicationic **ETTE** shows that whereas the outer C–O bond lengths remain unchanged (1.345 Å) the decrease of the length of the inner C–O bond to 1.328 Å suggests that the (−C=O$^+$−) mesomeric form (Scheme 4) contributes to delocalization of the positive charges. A similar effect is observed for the **TEET** dication, in which the inner C–O bond lengths (1.334 Å) are shorter than the outer ones (1.344 Å).

Field-effect thin-film transistor: The analysis of the hybrid oligomers as active materials in devices such as OFETs or solar cells requires a considerable effort in device elaboration and characterization which largely exceeds the scope of this article. However, to get a first insight into the potential of these compounds as semiconductors, a field-effect transistor was fabricated with **TETET** as active material. This compound was selected on the basis of its alternating TE structure, which is expected to lead to a rather homogeneous electronic distribution of its all-*anti* planar conformation with close packing of the molecules in the solid state.

Figure 7 shows the UV/Vis absorption spectrum of **TETET** in solution and as a thin film sublimed onto glass under high vacuum. As discussed above, the solution spec-

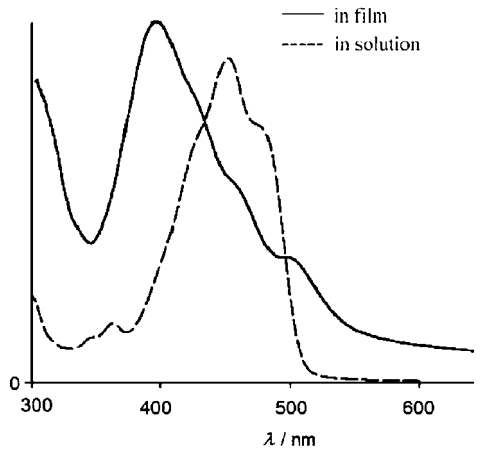

Figure 7. Electronic absorption spectrum of **TETET**. Dashed line: 10^{-5} M in CH_2Cl_2. Solid line: thin film sublimed onto glass (thickness 80 nm).

trum shows a fine structure with a maximum at 452 nm. The solid-state spectrum has a small band at 510 nm corresponding to the 0–0 transition and an intense new transition at 390 nm. Such behavior, already observed for oligothiophenes[21] and oligothienylenevinylenes,[22] has been attributed to exciton interactions between adjacent molecules in a close-packed arrangement. As already discussed for *n*Ts the coupling between transition dipoles of molecules at nonequivalent sites leads to Davydov splitting of the singlet excited state.[23]

The OFET was built with n-doped silicon as gate and thermally grown SiO_2 as dielectric. After sublimation of the organic semiconductor, gold source and drain electrodes were grown by sublimation on top of the organic film through a mask, leading to a channel of 50 μm length and 1 mm width. Figure 8 shows an AFM image of the **TETET** film deposited on the Si/SiO_2 substrate kept at a temperature of 80 °C. The film is composed of crystalline terraces organized layer by layer parallel to the substrate surface. The AFM cross-sec-

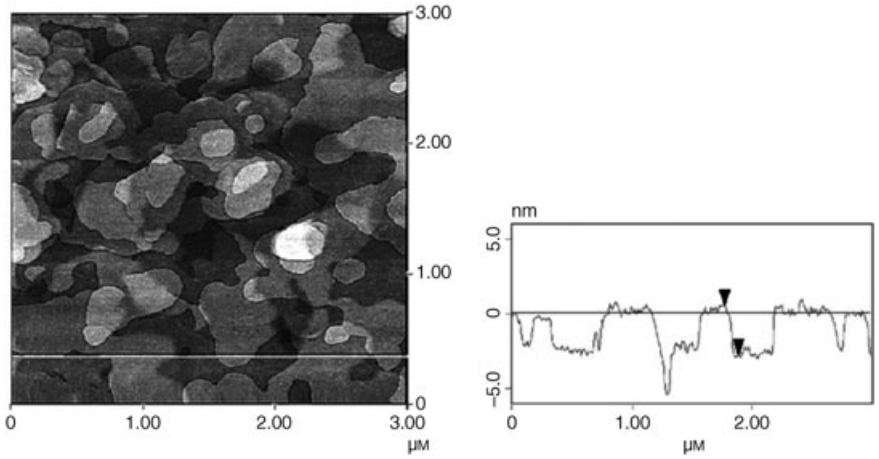

Figure 8. AFM picture of **TETET** vacuum-evaporated onto Si/SiO_2 substrate kept at a controlled temperature of 80 °C.

tion analysis of the molecular terraces revealed an average step size of 2.6 nm. Comparison of the height of the terraces with the estimated length of the **TETET** molecule (3.5 nm) suggests that the molecules are tilted at an angle of about 42° to the normal to the surface.

The FETs exhibit drain current I_d characteristics with well-defined linear and saturation regimes. The amplification mode of I_d takes place when negative gate voltage V_g increases, as expected for a p-type organic semiconductor (Figure 9). A field effect mobility μ_{FE} of $6\times10^{-4}\,cm^2\,V^{-1}\,s^{-1}$

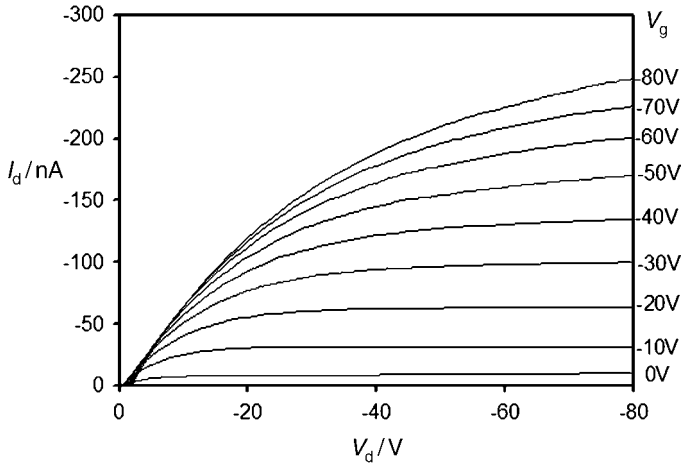

Figure 9. Drain current versus drain voltage characteristic for various source-gate voltages of an FET based on **TETET**.

was calculated from both linear and saturation current regimes with classical equations. The limited amount of material available did not allow any attempt to optimize the device performances. Therefore, these preliminary results should be considered as a bottom limit, and it seems likely that devices based on this compound have a substantial potential for improvement. Although still modest, the performances of this first device shows that hybrid T–E conjugated systems can function as organic semiconductors. Detailed investigations of the relationships between molecular structure and solid-state electronic properties and the potential of this new class of hybrid conjugated structures as organic semiconductors in devices such as OFETs and solar cells are underway.

Conclusion

Various series of hybrid oligothiophenes based on different combinations of thiophene and EDOT rings have been synthesized and characterized. The analysis of the relationships between the structure and the electronic properties of these oligomers by X-ray diffraction, optical and electrochemical techniques, and theoretical calculations shows that the self-rigidifying effect associated with noncovalent intramolecular S···O interactions observed for the tetrameric model system also occurs in longer EDOT-containing oligomers. For alternating EDOT–thiophene systems, these interactions contribute to stabilize a planar *anti* conformation of the thiophene rings with a coherence length extending up to the heptamer stage.

Experimental and theoretical results show that appropriate combination of this self-structuring effect with the strong electron-donor properties of the EDOT group allows a fine-tuning of the electronic properties of the neutral and charged states of hybrid oligothiophenes.

Although these various sets of results can have important implications for future use of EDOT-based functional π-conjugated systems as organic semiconductors, they also underline the difficulty of investigating structure–properties relationships in this class of oligomers due to the complexity of the interplay of intra- and interchain effects.

Nevertheless, the encouraging preliminary results obtained on the first OFET based on an EDOT-containing oligothiophene confirm the potential of this new class of organic semiconductors for device applications. The realization of OFETs and solar cells based on these novel materials is now underway and will be reported in future publications.

Experimental Section

General: NMR spectra were recorded with a Bruker Avance DRX 500 (^1H, 500.13 MHz and ^{13}C, 125.75 MHz) or a Jeol GSX 270WB (^1H, 270 MHz) instrument. Chemical shifts are given in ppm relative to TMS. MALDI-TOF MS spectra were recorded on Bruker Biflex-III apparatus, equipped with a 337 nm N_2 laser. The high-resolution mass spectra (HRMS), obtained by electronic impact (EI), fast atom bombardment

(FAB), or electrospray (ESI), were recorded on a double-focusing mass spectrometer Jeol JMS 700 with magneto-electrostatic analyzers. UV/Vis spectra were recorded on a Lambda 19 instrument.

The solvents were purified and/or dried according to the usual protocols. EDOT (**1**) was purchased from Bayer and was distilled under low pressure before use. Column chromatographic purifications were carried out on Merck silica gel Si 60 (40–63 μm). Melting points are uncorrected. Elemental analysis were performed by the Service Central d'Analyses du CNRS (Vernaison, France).

Cyclic voltammetry was performed in dichloromethane purchased from SDS (HPLC grade). Tetrabutylammonium hexafluorophosphate (0.1 or 0.2 M as supporting electrolyte) was purchased from Acros and used without purification. Solutions were deaerated by nitrogen bubbling prior to all experiments, which were run under a nitrogen atmosphere. Experiments were done in a one-compartment cell equipped with a platinum working microelectrode (∅ 1 mm) and a platinum wire counterelectrode. An Ag/AgCl electrode, checked against the ferrocene/ferricinium couple (Fc/Fc^+) before and after each experiment, was used as reference. Electrochemical experiments were carried out with a PAR 273 potentiostat with positive feedback compensation.

The synthetic procedures for the intermediate compounds are described in the Supporting Information.

General procedure for Stille coupling

Preparation of the stannyl derivatives: *n*BuLi (2.5 or 1.6 M in hexane) was added dropwise to a solution containing the thiophene derivative dissolved in dry THF under inert atmosphere (N_2). The mixture was stirred for 1 h at the addition temperature. Then tributyltin chloride was added dropwise and the mixture was stirred at the same temperature for 30 min before allowing it to warm to room temperature. After dilution with diethyl ether, the organic phase was successively washed with a saturated solution of $NaHCO_3$ then with water. After drying over $MgSO_4$, the solvent was evaporated and the product was used without further purification in the following reactions.

Coupling reaction: The stannyl derivative, the brominated derivative, and the catalyst (5% $[Pd(PPh_3)_4]$) were refluxed in dry toluene (50 mL) for 12 h under inert atmosphere (N_2). After concentration, the residue was dissolved in CH_2Cl_2. The organic phase was washed twice with a saturated solution of $NaHCO_3$ then with water. After drying over $MgSO_4$ and evaporation of solvent, the product was purified by the appropriate method.

3,4,3‴,4‴-Bis(ethylenedioxy)-5,5‴-dihexyl-2,2′:5′,2″:5″,2‴-quaterthiophene (ETTE): Stannyl derivative **7b** was prepared from **7a**. Stille coupling was done according to the general procedure by using 5,5′-dibromo-2,2′-bithiophene (860 mg, 2.65 mmol), **7b** (6.62 mmol, 2.5 equiv), and $[Pd(PPh_3)_4]$ (300 mg). The product was purified by chromatography on silica gel (CH_2Cl_2/ether petroleum (EP) 1/1) to give **ETTE** as an orange solid (920 mg, 56%).

ETTE: M.p. 126 °C; ^{1}H NMR ($CDCl_3$): $\delta = 0.89$ (t, $^3J = 6.9$ Hz, 6H), 1.34 (m, 12H), 1.6 (m, 4H), 2.64 (t, $^3J = 7.6$ Hz, 4H), 4.23 (m, 4H), 4.33 (m, 4H), 7.01 (d, $^3J = 3.8$ Hz, 2H), 7.03 ppm (d, $^3J = 3.8$ Hz, 2H); ^{13}C NMR ($CDCl_3$): $\delta = 14.05$, 22.54, 25.71, 28.75, 30.32, 31.50, 64.47, 65.09, 107.92, 116.44, 122.44, 123.03, 133.72, 134.94, 137.37, 137.52 ppm; HRMS calculated for $C_{32}H_{38}O_4S_4$: 614.1653; found: 614.1642; elemental analysis calcd (%) for $C_{32}H_{38}O_4S_4$: C 62.50, H 6.23, O 10.41, S 20.86; found: C 62.29, H 6.10, O 10.51, S 20.59.

3′,4′,3″,4″-Bis(ethylenedioxy)-5,5‴-dihexyl-2,2′:5′,2″:5″,2‴-quaterthiophene (TEET): Distannyl derivative **5c** was prepared from **5a** by using two equivalents of *n*BuLi and a slight excess of Bu_3SnCl. Stille coupling was done according to the general procedure by using 2-bromo-5-hexylthiophene (11.75 mmol, 1.5 equiv) **5c** (4.7 mmol), and $[Pd(PPh_3)_4]$ (500 mg). The product was purified by chromatography on silica gel (CH_2Cl_2/EP 1/1) to give **TEET** as an orange solid (1.41 g, 56%).

TEET: M.p. 150 °C; ^{1}H NMR ($CDCl_3$): $\delta = 0.88$ (t, $^3J = 6.9$ Hz, 6H), 1.34 (m, 12H), 1.67 (m, 4H), 2.79 (t, $^3J = 7.4$ Hz, 4H), 4.38 (m, 8H), 6.68 (d, $^3J = 3.5$ Hz, 2H), 7.03 ppm (d, $^3J = 3.5$ Hz, 2H); ^{13}C NMR ($CDCl_3$): $\delta =$ 14.07, 22.56, 28.77, 30.11, 31.56, 31.61, 64.93, 65.03, 106.95, 110.65, 122.28, 124.16, 132.13, 136.48, 136.91, 144.57 ppm; HRMS calculated for $C_{32}H_{38}O_4S_4$: 614.1653; found: 614.1652; elemental analysis calcd (%) for $C_{32}H_{38}O_4S_4$: C 62.50, H 6.23, O 10.41; found: C 62.76, H 6.11, O 10.45.

3,4,3″,4″-Bis(ethylenedioxy)-5,5‴-dihexyl-2,2′:5′,2″:5″,2‴-quaterthiophene (TETE): Stille coupling was done according to the general procedure by using **7b** (1.70 mmol), **8b** (500 mg, 0.65 mmol), and $[Pd(PPh_3)_4]$ (80 mg). The product was purified by chromatography on silica gel (CH_2Cl_2/EP 2/1) to give **TETE** as an orange solid (80 mg, 10%).

TETE: M.p. 98 °C; ^{1}H NMR ($CDCl_3$): $\delta = 0.89$ (m, 6H), 1.32 (m, 12H), 1.65 (m, 4H), 2.63 (t, $^3J = 7.5$ Hz, 2H), 2.79 (t, $^3J = 7.5$ Hz, 2H), 4.23 (m, 2H), 4.32 (m, 2H), 4.38 (s, 4H), 6.68 (d, $^3J = 3.5$ Hz, 1H), 7.00–7.10 ppm (m, 3H); MS (MALDI) calcd for $C_{32}H_{38}O_4S_4$: 614.17; found: 614.04; elemental analysis calcd (%) for $C_{32}H_{38}O_4S_4$: C 62.50, H 6.23, O 10.41; found: C 62.35, H 6.10, O 10.52.

3,4,3‴,4‴-Bis(ethylenedioxy)-5,5‴-dihexyl-2,2′:5′,2″:5″,2‴:5‴,2⁗-quinquithiophene (ETTTE): Stille coupling was done according to the general procedure by using **7b** (1.05 mmol), dibromoterthiophene (200 mg, 0.49 mmol), and $[Pd(PPh_3)_4]$ (60 mg). The product was purified by chromatography on silica gel (CH_2Cl_2/EP 1/1) to give **ETTTE** as an orange solid (30 mg, 18%).

ETTTE: M.p. 131 °C; ^{1}H NMR ($CDCl_3$): $\delta = 0.9$ (t, $^3J = 6.8$ Hz, 6H), 1.33 (m, 12H), 1.60 (m, 4H), 2.64 (t, $^3J = 7.4$ Hz, 4H), 4.24 (m, 4H), 4.33 (m, 4H), 7.00–7.06 ppm (m, 6H); MS (MALDI-TOF) calcd for $C_{36}H_{40}O_4S_5$: 696.15; found: 696.04; elemental analysis calcd (%) for $C_{36}H_{40}O_4S_5$: C 62.03, H 5.78, O 9.18, S 23.00; found: C 61.74, H 5.79, O 8.97, S 22.88.

3′,4′,3‴,4‴-Bis(ethylenedioxy)-5,5⁗-dihexyl-2,2′:5′,2″:5″,2‴:5‴,2⁗:5⁗,2⁗′-quinquithiophene (TETET): Stannyl derivative **3b** was prepared from **3a**. Stille coupling was done according to the general procedure by using **3b** (1.83 mmol), 2,5-dibromothiophene (200 mg, 0.85 mmol), and $[Pd(PPh_3)_4]$ (100 mg). The product was purified by chromatography on silica gel (CH_2Cl_2/EP 2/1) and then recrystallized from $CHCl_3$/absolute ethanol to give **TETET** as an orange solid (355 mg, 62%).

TETET: M.p. 188 °C; ^{1}H NMR ($CDCl_3$): $\delta = 0.9$ (t, $^3J = 6.8$ Hz, 6H), 1.34 (m, 12H), 1.68 (m, 4H), 2.79 (t, $^3J = 7.5$ Hz, 4H), 4.39 (m, 8H), 6.69 (d, $^3J = 3.5$ Hz, 2H), 7.03 (d, $^3J = 3.5$ Hz, 2H), 7.12 ppm (s, 2H); ^{13}C NMR ($CDCl_3$): $\delta = 14.07$, 22.56, 28.76, 30.10, 31.55, 31.56, 64.90, 64.97, 109.10, 109.95, 122.64, 122.79, 124.23, 131.77, 132.84, 136.92, 137.42, 144.93 ppm; HRSM calcd for $C_{36}H_{40}O_4S_5$: 696.1530; found: 696.1531; elemental analysis calcd (%) for $C_{36}H_{40}O_4S_5$: C 62.03, H 5.78, O 9.18, S 23.00; found: C 61.97, H 5.68, O 8.71, S 23.46.

5,5⁗-Dihexyl-3′,4′,3″,4″,3‴,4‴-tris(ethylenedioxy)-2,2′:5′,2″:5″,2‴:5‴,2⁗:5⁗,2⁗′-quinquithiophene (TEEET): Stille coupling was done according to the general procedure by using **3b** (2.86 mmol), 2,5-dibromo-3,4ethylenedioxythiophene (400 mg, 1.33 mmol), and $[Pd(PPh_3)_4]$ (160 mg). The product was purified by chromatography on silica gel (CH_2Cl_2/EP 1/1, 1% Et_3N) to give **TEEET** as a red solid (210 mg, 21%).

TEEET: M.p. 212 °C; ^{1}H NMR ($CDCl_3$): $\delta = 0.89$ (t, $^3J = 6.4$ Hz), 1.32 (m, 12H), 1.68 (m, 4H), 2.79 (t, $^3J = 7.5$ Hz, 4H), 4.4 (m, 12H), 6.67 (d, $^3J =$ 3.4 Hz, 2H), 7.03 ppm (d, $^3J = 3.4$ Hz, 2H); HRMS calcd for $C_{38}H_{42}O_6S_5$: 754.1585; found: 754.1548; elemental analysis calcd (%) for $C_{38}H_{42}O_6S_5$: C 60.45, H 5.61, O 12.71, S 21.23; found: C 60.21, H 5.70, O 12.99, S 21.13.

5,5⁗-Dihexyl-3,4,3″,4′,3‴,4⁗-tris(ethylenedioxy)-2,2′:5′,2″:5″,2‴:5‴,2⁗:5⁗,2⁗′-quinquithiophene (ETETE): Stille coupling was done according to the general procedure by using **4b** (600 mg, 1.29 mmol), **7b** (2.8 mmol), and $[Pd(PPh_3)_4]$ (150 mg). The product was purified by chromatography on silica gel (CH_2Cl_2/EP 1/1) to give **ETETE** as a red solid (490 mg, 47%). **ETETE**: M.p. 214 °C; ^{1}H NMR ($CDCl_3$): $\delta = 0.89$ (t, $^3J = 6.8$ Hz, 6H), 1.32 (m, 12H), 1.61 (m, 4H), 2.63 (t, $^3J = 7.4$ Hz, 4H), 4.2 (m, 4H), 4.32 (m, 4H), 4.39 (s, 4H), 7.05 (d, $^3J = 3.8$ Hz, 2H), 7.09 ppm (d, $^3J = 3.8$ Hz, 2H); ^{13}C NMR ($CDCl_3$): $\delta = 14.09$, 22.57, 25.74, 28.79, 30.36, 31.53, 64.51, 64.96, 65.11, 108.13, 109.55, 116.27, 122.05, 122.83, 132.03, 133.71, 137.28 (2), 137.56 ppm; HRMS calculated for $C_{38}H_{42}O_6S_5$: 754.1585; found: 754.1574; elemental analysis calculated (%) for $C_{38}H_{42}O_6S_5$: C 60.45, H 5.61, O 12.71, S 21.23; found: C 60.22, H 5.65, O 13.28, S 21.08.

5,5⁗-Dihexyl-3,4,3′,4′3‴,4‴,3⁗,4⁗-tetrakis(ethylenedioxy)-2,2′:5′,2″:5″,2‴:5‴,2⁗:5⁗,2⁗′-quinquithiophene (EETEE): Stannyl derivative **5b** was prepared from **5a**. Stille coupling was done according to the general

procedure by using **5b** (0.94 mmol), 2,5-dibromothiophene (106 mg, 0.44 mmol), and $[Pd(PPh_3)_4]$ (25 mg). The product was purified by chromatography on silica gel (CH_2Cl_2/EP 1/1, Et_3N 1%) to give **EETEE** as a red solid (70 mg, 20%).

EETEE: M.p. 225°C; ^{1}H NMR ($CDCl_3$): $\delta = 0.88$ (t, $^3J = 6.8$ Hz, 6H), 1.31 (m, 12H), 1.6 (m, 4H), 2.64 (t, $^3J = 7$ Hz, 4H), 4.23 (m, 4H), 4.32 (m, 4H), 4.38 (s, 8H), 7.11 (s, 2H); Solubility was too low to measure the ^{13}C NMR spectrum. HRMS calculated for $C_{40}H_{44}O_8S_5$: 812.16397; found: 812.1635.

5,5‴″-Dihexyl-3,4,3‴,4‴,3‴″,4‴″-tris(ethylenedioxy)-2,2′:5′,2″:5″,2‴:5‴,2‴″:5‴″,2‴″″:5‴″″,2‴″″″-septithiophene (TETETET): Stille coupling was done according to the general procedure by using **4b** (450 mg, 0.97 mmol), **3b** (2.08 mmol), and $[Pd(PPh_3)_4]$ (120 mg). The product was purified by Soxhlet extraction with diethyl ether to remove impurities and then acetone to obtain **ETETETE** as a red powder (120 mg, 14%). The poor solubilty of the product prevented NMR spectroscopy. M.p. > 300°C; MS (MALDI-TOF) calculated for $C_{46}H_{46}O_6S_7$: 918.14; found: 918.00.

X ray structures: Data were collected at 293 K on an Enraf-Nonius MACH3 four-circle diffractometer for **ETTE** and on a STOE-IPDS diffractometer for **TEET**, both equipped with a graphite monochromator utilizing $Mo_{K\alpha}$ radiation ($\lambda = 0.71073$ Å). The structures were solved by direct methods (SIR) and refined on F by full-matrix least-squares techniques using MolEN package programs for **ETTE** and by full-matrix least-squares methods on F^2 with SHELXL97 for **TEET**.

*Crystal data and structure refinement for **ETTE***: $C_{16}H_{19}O_2S_2$, $M_r = 307.43$, yellow prism, $1.00 \times 0.31 \times 0.12$ mm, triclinic, $P\bar{1}$, $a = 12.316(1)$, $b = 12.264(2)$, $c = 12.556(1)$ Å, $\alpha = 67.95(1)$, $\beta = 68.025(8)$, $\gamma = 67.804(9)$°, $V = 1566.7(3)$ Å^3, $Z = 2$, $T = 294$ K, $\rho_{calcd} = 1.30$ g cm^{-3}, 5795 reflections collected in the range $\theta = 2.5$–25.0°, 5519 independent reflections, of which 1490 with $I > 3\sigma(I)$ converged to $R = 0.097$ and w$R2 = 0.131$ with 201 parameters, GOF = 2.435. S and O atoms were refined anisotropically, and H atoms were included in the calculation without refinement.

*Crystal data and structure refinement for **TEET***: $C_{16}H_{19}O_2S_2$, $M_r = 307.43$, yellow plate, $0.46 \times 0.40 \times 0.03$ mm, monoclinic, $P2_1/n$, $a = 12.835(2)$, $b = 8.6701(8)$, $c = 15.097(2)$ Å, $\beta = 113.67(2)$°, $V = 1538.7(3)$ Å^3, $Z = 4$, $T = 293$ K, $\rho_{calcd} = 1.327$ g cm^{-3}, 11740 reflections collected in the range $\theta = 1.8$–25.8°, 2868 independent reflections, of which 1400 with $I > 2\sigma(I)$ converged to $R = 0.054$ and w$R2 = 0.112$ with 181 parameters, GOF = 0.836. All non-H atoms were refined anisotropically, and the H atoms were included in the calculation without refinement. Absorption was corrected by the multiscan technique.

CCDC-252647 and CCDC-252648 contain the supplementary crystallographic data for this paper. These data can be obtained free of charge from The Cambridge Crystallographic Data Centre via www.ccdc.cam.ac.uk/data_request/cif.

[1] a) C. D. Dimitrakopoulos, P. R. L. Malenfant, *Adv. Mater.* **2002**, *14*, 99; b) J. A. Rogers, Z. Bao, A. Dodabalapur, B. Crone, V. R. Raju, H. E. Katz, V. Kuck, K. J. Ammundson, P. Drzaic, *Proc. Natl. Acad. Sci. USA Proc. Natl. Acad. Eng.* **2001**, *98*, 4817; c) F. Garnier, *Acc. Chem. Res.* **1999**, *32*, 209; d) G. Horowitz, *Adv. Mater.* **1998**, *10*, 3; e) H. E. Katz, *J. Mater. Chem.* **1997**, *7*, 369; f) G. Barbarella, M. Zambianchi, L. Antolini, P. Ostoja, P. Maccagnani, A. Bongini, E. A. Marseglia, E. Tedesco, G. Gigli, R. Cingolani, *J. Am. Chem. Soc.* **1999**, *121*, 8920; g) M. Halik, H. Klauk, U. Zschieschang, G. Schmid, S. Ponomarenko, S. Kirchmeyer, W. Weber, *Adv. Mater.* **2003**, *15*, 917.

[2] a) U. Mitschke, P. Bauerle, *J. Mater. Chem.* **2000**, *10*, 1471; b) F. Geiger, M. Stoldt, R. Schweiser, P. Bäuerle, E. Umbach, *Adv. Mater.* **1993**, *5*, 922; c) G. Barbarella, L. Favaretto, G. Sotgiu, P. Zambianchi, A. Bongini, C. Arbizzani, M. Mastragostino, M. Anni, G. Gigli, R. Cingolani, *J. Am. Chem. Soc.* **2000**, *122*, 11971; d) G. Barbarella, L. Favaretto, G. Sotgiu, L. Antolini, G. Gigli, R. Cingolani, A. Bongini, *Chem. Mater.* **2001**, *13*, 4112.

[3] a) C. Videlot, A. El Kassmi, D. Fichou, *Solar Energy Materials & Solar Cells* **2000**, *63*, 69; b) R. de Bettignies, Y. Nicolas, P. Blanchard, E. Levillain, J.-M. Nunzi, J. Roncali, *Adv. Mater.* **2003**, *15*, 1939.

[4] J. Cornil, J. P. Calbert, D. Beljonne, R. Silbey, J-L. Brédas, *Adv. Mater.* **2000**, *12*, 978.

[5] J. Roncali, *Chem. Rev.* **1997**, *97*, 173.

[6] B. L. Groenendaal, F. Jonas, D. Freitag, D. Pielartzik, J. R. Reynolds, *Adv. Mater.* **2000**, *12*, 481.

[7] a) S. Akoudad, J. Roncali, *Chem. Commun.* **1998**, 2081; b) S. Akoudad, J. Roncali, *Synth. Met.* **1999**, *101*, 149; c) I. Perepichka, E. Levillain, J. Roncali, *J. Mater. Chem.* **2004**, *14*, 1679.

[8] a) J. M. Raimundo, P. Blanchard, P. Frère, N. Mercier, I. Ledoux Rak, R. Hierle, J. Roncali, *Tetrahedron Lett.* **2001**, *42*, 150; b) J. M. Raimundo, P. Blanchard, N. Gallego Planas, N. Mercier, I. Ledoux Rak, R. Hierle, *J. Org. Chem.* **2002**, *67*, 205.

[9] a) S. Akoudad, P. Frère, N. Mercier, J. Roncali, *J. Org. Chem.* **1999**, *64*, 4267; b) P. Leriche, M. Turbiez, V. Monroche, P. Frère, P. Blanchard, P. J. Skabara, J. Roncali, *Tetrahedron Lett.* **2003**, *44*, 649.

[10] a) S. Akoudad, J. Roncali, *Synth. Met.* **1998**, *93*, 114; b) G. A. Sotzing, J. R. Reynolds, P. J. Steel, *Adv. Mater.* **1997**, *9*, 795.

[11] G. A. Sotzing, J. R. Reynolds, P. J. Steel, *Chem. Mater.* **1996**, *8*, 882.

[12] a) R. G. Hicks, M. B. Nodwell, *J. Am. Chem. Soc.* **2000**, *122*, 6746; b) J. J. Apperloo, L. Groenendaal, H. Verheyen, M. Jayakannan, R. A. J. Janssen, A. Dkhissi, D. Beljonne, R. Lazzaroni, J. L. Brédas, *Chem. Eur. J.* **2002**, *8*, 2384; c) M. Turbiez, P. Frère, J. Roncali, *J. Org. Chem.* **2003**, *68*, 5357.

[13] a) A. K. Mohanakrishnan, A. Hucke, M. A. Lyon, M. V. Lakshmikantham, M. P. Cava, *Tetrahedron* **1999**, *55*, 11745; b) M. Turbiez, P. Frère, P. Blanchard, J. Roncali, *Tetrahedron Lett.* **2000**, *41*, 5521.

[14] J. Kagan, S. K. Arora, *Heterocycles* **1983**, *20*, 1937.

[15] H. Meng, D. F. Perepichka, F. Wudl, *Angew. Chem.* **2003**, *115*, 682; *Angew. Chem. Int. Ed.* **2003**, *42*, 658.

[16] F. Garnier, R. Hajlaoui, A. El Kassmi, G. Horowitz, L. Laigre, W. Porzio, M. Armanini, F. Provasoli, *Chem. Mater.* **1998**, *10*, 3334.

[17] a) S. D. D. V. Rughooputh, S. Hotta, A. J. Heeger, F. Wudl, *J. Polym. Sci.* **1987**, *25*, 1071; b) O. Inganäs, W. Salaneck, J. E. Osterholm, J. Laakso, *Synth. Met.* **1988**, *22*, 395.

[18] Gaussian 98 (Revision A.9), M. J. Frisch, G. W. Trucks, H. B. Schlegel, G. E. Scuseria, M. A. Robb, J. R. Cheeseman, V. G. Zakrzewski, J. A. Jr. Montgomery, R. E. Stratmann, J. C. Burant, S. Dapprich, J. M. Millam, A. D. Daniels, K. N. Kudin, M. C. Strain, O. Farkas, J. Tomasi, V. Barone, M. Cossi, R. Cammi, B. Mennucci, C. Pomelli, C. Adamo, S. Clifford, J. Ochterski, G. A. Petersson, P. Y. Ayala, Q. Cui, K. Morokuma, D. K. Malick, A. D. Rabuck, K. Raghavachari, J. B. Foresman, J. Cioslowski, J. V. Ortiz, A. G. Baboul, B. B. Stefanov, G. Liu, A. Liashenko, P. Piskorz, I. Komaromi, R. Gomperts, R. L. Martin, D. J. Fox, T. Keith, M. A. Al-Laham, C. Y. Peng, A. Nanayakkara, C. Gonzalez, M. Challacombe, P. M. W. Gill, B. G. Johnson, W. Chen, M. W. Wong, J. L. Andres, M. Head-Gordon, E. S. Replogle and J. A. Pople Gaussian, Inc., Pittsburgh, PA, **1998**.

[19] A. Dkhissi, D. Beljonne, R. Lazzaroni, F. Louwet, L. Groenendaal, J. L. Brédas, *Int. J. Quantum Chem.* **2003**, *91*, 517.

[20] T. Nishinaga, A. Wakamiya, D. Yamazaki, K. Komatsu, *J. Am. Chem. Soc.* **2004**, *126*, 3163.

[21] F. Garnier, A. Yassar, R. Hajlaoui, G. Horowitz, F. Deloffre, B. Servet, S. Ries, P. Alnot, *J. Am. Chem. Soc.* **1993**, *115*, 8716.

[22] C. Videlot, J. Ackermann, P. Blanchard, J-M. Raimundo, P. Frère, M. Allain, R. de Bettignies, E. Levillain, J. Roncali, *Adv. Mater.* **2003**, *15*, 306.

[23] A. Yassar, G. Horowitz, P. Valat, V. Wintgens, M. Hmyene, F. Deloffre, P. Srivastava, P. Lang, F. Garnier, *J. Phys. Chem.* **1995**, *99*, 9155.

Received: October 18, 2004
Revised: January 30, 2005
Published online: April 14, 2005